J Mater Sci (2011) 46:131–135
DOI 10.1007/s10853-010-4865-x

Fe–Ga–As precipitates and their magnetic domain structures in high-dose iron implanted GaAs

Nathan Taylor · Kai Sun

Received: 17 April 2010 / Accepted: 23 August 2010 / Published online: 3 September 2010

Abstract The integration of ferromagnetism with semiconductors to fabricate ferromagnetic semiconductors has been believed to be a potential way to make new spintronic devices. We have synthesized ferromagnetic $Fe_3Ga_{2-x}As_x$ nanoparticles in the surface of GaAs by employing ion implantation and rapid thermal annealing processes. Transmission electron microscopy revealed that these nanoparticles exist only in the top surface of the GaAs samples, with sizes from several to hundreds of nanometers. They have two orientation relationships to the GaAs matrix: $[1-210]_p//[011]_m$, $(10-10)_p//(-42-2)_m$ and $(0002)_p//(11-1)_m$; and $[1-210]_p//[011]_m$, $(-1010)_p//(42-2)_m$ and $(0002)_p//(-11-1)_m$. The magnetic structures of the precipitates were studied by magnetic force microscopy. Results indicate that most of the ferromagnetic nanoparticles have single magnetic domains with their magnetic poles randomly orientated.

Introduction

The combination of magnetism along with the electronic properties of semiconductors, i.e., the fabrication of ferromagnetic semiconductors, has been receiving extensive attentions over the past two decades [1, 2]. This is because that the ferromagnetic semiconductors are believed to have potential applications in new classes of devices such as logic circuits, memory storage, optical communications, quantum computing devices, etc [3–5]. Transition metal (TM) atoms like Fe, Co, Ni, and Mn can introduce spins in the semiconductors when either doped into the semiconductor or alloyed with one or two composition components of the semiconductor [6–11]. Thus, different methods have been used to introduce TM atoms into different semiconductor materials. Among which, ion implantation is very unique that can be used to introduce any metal ions into any semiconductors regardless the solubility of the metal in the semiconductor substrate. Therefore, it has been playing a very important role in the development of spintronics [6–11].

The Fe/GaAs system is among the metal/semiconductor systems that have been widely studied [6, 12–14]. Fe was combined with GaAs either as thin films grown on GaAs single crystal substrates or doped in GaAs matrices mainly through ion implantation. An annealing process was normally involved that induced the formation of ferromagnetic phases. Among which, the $Fe_3Ga_{2-x}As_x$ phase was considered as a promising candidate for epitaxial and thermodynamically stable contacts on GaAs. Thus, high quality thin films of the phase have been grown on GaAs, and its magnetic properties at different temperatures have been extensively studied [15–19]. Nevertheless, there is still no report on the study of the magnetic domain structures of the precipitates in the literature. There are many ways to observe magnetic domains. Magnetic force microscopy (MFM) is a useful qualitative characterization tool in the development of thin-film semiconductor spintronics devices because it can be used to image and measure magnetization properties of magnetic materials [20].

In this study, high-dose Fe ions were implanted into GaAs and then rapid thermal annealing (RTA) was performed at a high temperature on the sample. Phases formed in the implanted layers were studied by transmission electron microscopy (TEM) and the surface morphology

N. Taylor · K. Sun (✉)
Department of Materials Science and Engineering, University of Michigan, Ann Arbor, MI 48109, USA
e-mail: kaisun@umich.edu

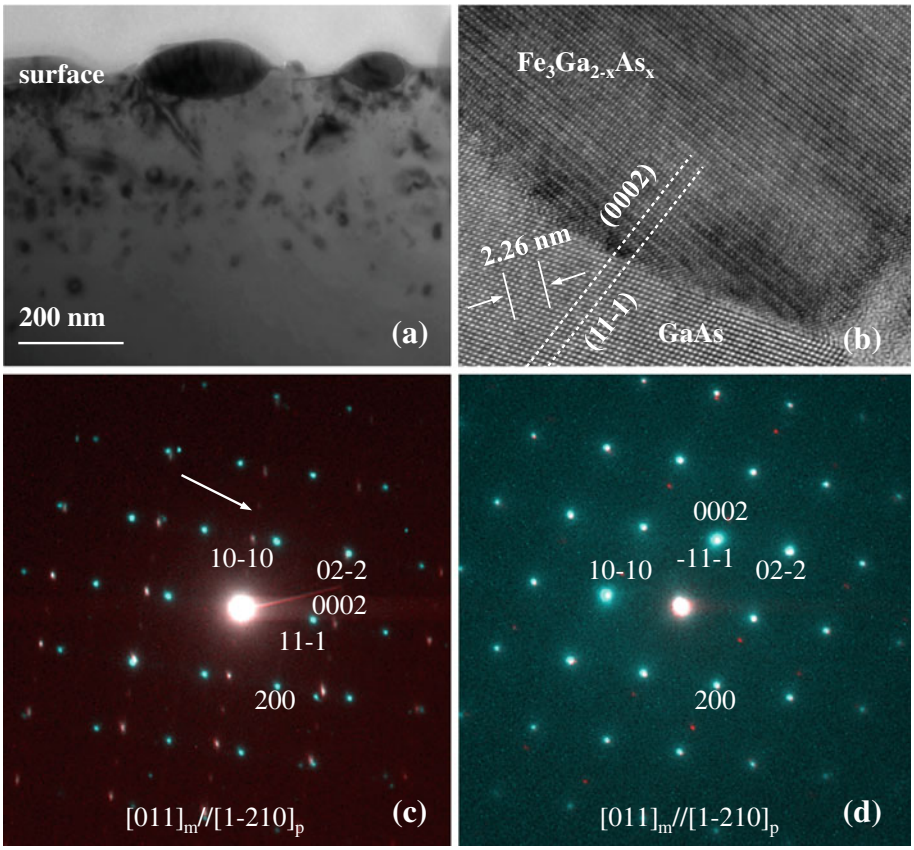

Fig. 1 **a** Cross-sectional TEM BF image showing the formation of nanoparticles in the surface of GaAs; **b** HREM image taken from the $Fe_3Ga_{2-x}As_x$ precipitate and the GaAs matrix; **c**, **d** SAED patterns indicating the orientation relationships between the precipitate and the GaAs matrix

and magnetic domain structures of the sample were further studied by atomic force microscopy (AFM) and MFM.

Experimental

Single crystal (001) SI-GaAs wafers were implanted with Fe ions at a dose of 1×10^{17} Fe^+/cm^2. The implantation was accomplished using a MEVVA 80 implanter in the broad beam mode with a beam size of several centimeters. The ion energy was kept at around 100 keV and the beam current at 5.0–7.0 mA/cm^2. During implantation, the GaAs wafers were not deliberately heated, though some of them were rapidly thermal-annealed afterward at 850 °C for 60 s. The cooling rate from the annealing temperature to room temperature was about 100 °C/s. Cross-sectional specimens cutting from these wafers used for TEM analysis were prepared by mechanical grinding, polishing, and argon ion-milling. The TEM study was carried out in a JEOL 2010F electron microscope with a point resolution of 0.23 nm.

Atomic force microscopy and MFM experiments were performed on a Digital Instruments Nanoscope IIIa at room temperature. The sample was not magnetized, and no magnetic field was applied during MFM imaging. A Si tip was used for AFM imaging performed at the tapping mode. For MFM imaging, a Si tip coated with Co–Cr alloy was used that was magnetized vertically under a magnetic field of 2,000 Oe. The lift heights used were from 30 to 100 nm.

Results and discussions

Figure 1a is TEM bright-field (BF) image showing the formation of small particles in the surface of the Fe implanted and annealed GaAs. Besides the precipitates, there formed also lots of defects such as dislocations and dislocations loops through the whole ion implanted range (~400 nm) even the sample have been annealed at high temperature. Our previous study indicated that there were not visible particles formed in the implanted layers before annealing [21]. Figure 1b is high-resolution electron microscopy (HREM) image taken from a precipitate together with the GaAs matrix. Figure 1c, d is two typical SAED patterns taken from the precipitates and the GaAs matrix. In all the two SAED patterns, diffraction spots with higher intensities are from the GaAs substrate and those with lower intensities are from the precipitates. Selected area electron diffraction patterns taken from the precipitates can be indexed using the reported $Fe_3Ga_{2-x}As_x$ phase with a NiAs structure ($P6_3/mmc$, $a = 0.402$ nm and $c = 0.503$ nm) [15–19]. Using the GaAs substrate as a reference, the

calculated d-spacing of (10 − 10) and (0002) are 0.345 nm (0.3481 nm) and 0.252 nm (0.2515 nm), respectively, which are slightly different from those in the parenthesis calculated according to the reported structure. X-ray energy dispersive spectroscopy analysis indicates the precipitates contains higher Ga and As which may be due to the scatter from the GaAs matrix. By indexing the composite SAED patterns as shown in Fig. 1c, d, we got two different

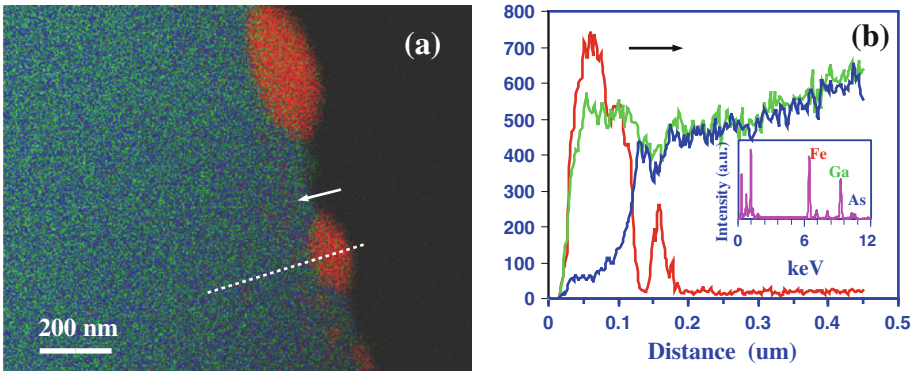

Fig. 2 **a** EDS element map generated from Fe (*red*), Ga (*green*), and As (*blue*) maps showing the distribution of Fe in the implanted layer of the GaAs matrix; **b** Ga, Fe, and As element profiles along the *dotted line* marked in (**a**). The *inset* in **b** is a typical EDS spectrum collected from the precipitate (Color figure online)

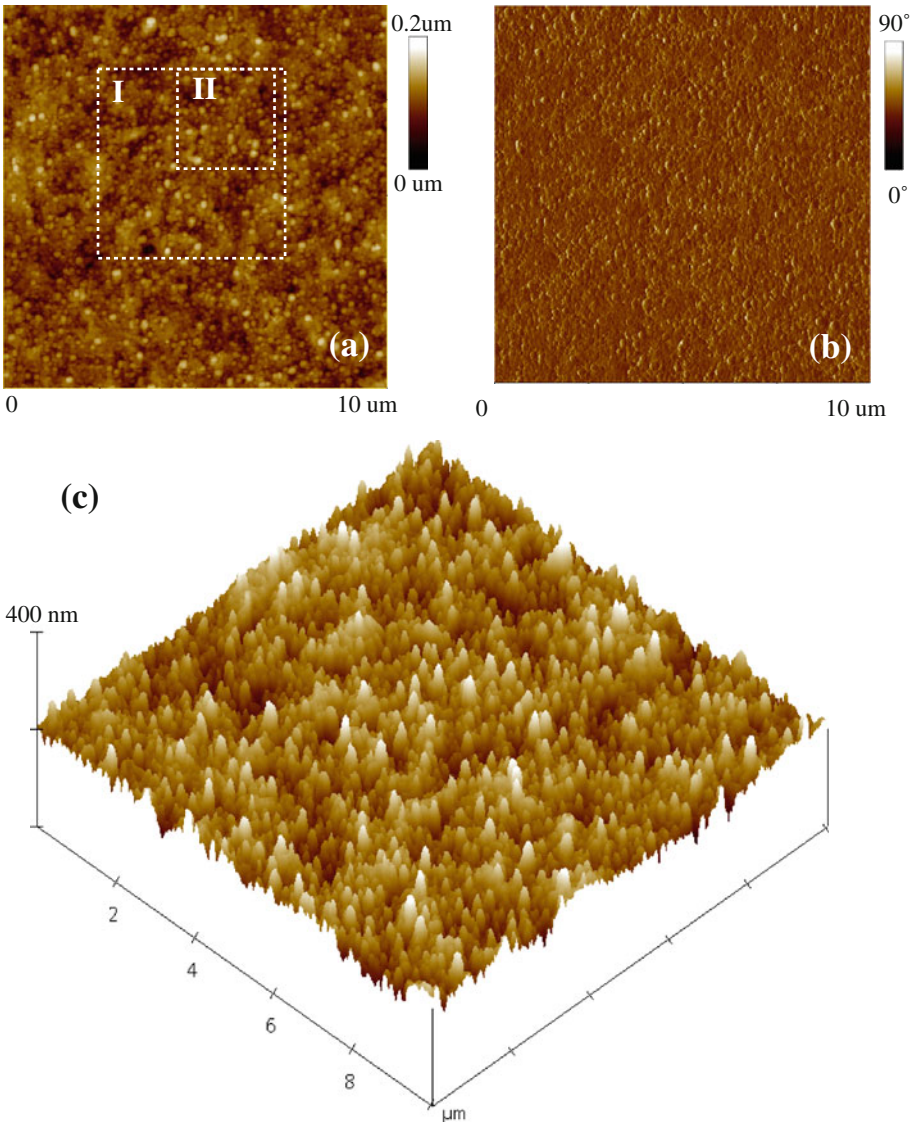

Fig. 3 AFM images acquired from the sample, **a** AFM height, **b** phase image, and **c** side-view height images, respectively (the set-point was set to be 0.8598 V)

orientation relationships between the precipitates (p) and the GaAs matrix (m). They are $[1-210]_p//[011]_m$, $(10-10)_p//(-42-2)_m$ and $(0002)_p//(11-1)_m$, or $[1-210]_p//[011]_m$, $(-1010)_p//(42-2)_m$ and $(0002)_p//(-11-1)_m$. They are slightly different from that reported by Chang et al. [6]. This is understandable due the equality between the (11−1) and (−11−1) and (42−2) and (−42−2) planes for the face-centered cubic structure and between the (−1010) and (10−10) planes for the hexagonal structure. As Chang et al. mentioned that the relationship is common for a hexagonal precipitate embedded in a cubic matrix because it provides the lowest strain due to the excellent match between the $(10-10)_p$ ($d = 0.3481$ nm) and the projection of $(002)_m$ on $(111)_m$ ($d = 0.3462$ nm) [6]. The lowest strain between the precipitate and the matrix can also be attributed to the excellent match between the $(111)_m$ and $(0002)_p$ planes because $3 \times d(111)_m$ (3×0.3264 nm $= 9.79$ nm) is close to $4 \times d(0002)_p$ ($4 \times 0.252 = 1.008$ nm). This relationship was outlined in Fig. 1b by two paralleling dotted lines. Extra diffraction spots were also observed at 1/2(10−10) positions (with one indicated by an arrow) in the SAED patterns shown in Fig. 1b, c but not in the pattern in Fig. 1d. These extra spots are from the ordered $Fe_3Ga_{2-x}As_x$ phase according to the literature [6, 18]. This indicates both $Fe_3Ga_{2-x}As_x$ and its ordered phases were formed in the Fe ion implanted and annealed GaAs. Some other extra spots along (0002) direction in the inserted SAED pattern in Fig. 1b are double diffractions from the GaAs and the precipitate overlapped areas. They cannot be attributed to the ordering along the [0002] direction of the precipitate as in the case of the reference [6].

Figure 2a shows Fe, Ga, and As distributions within the ion implanted layer. It indicates that Fe only exists within the top 200 nm range that was also confirmed by element profile analysis as shown in Fig. 2b. The inset in Fig. 2b is typical EDS spectrum collected from the precipitate. The difference between the depth distributions of Fe in GaAs from that reported in [6] is that the ion beam generated from a MEVVA source contains a mixture of several different charge states (Fe^+, Fe^{2+}, and Fe^{3+}) and so has a broad energy spectrum producing a relatively flat implantation depth profile.

Figure 3 is AFM images collected from the surface of the ion implanted and annealed GaAs sample. These images show that the $Fe_3Ga_{2-x}As_x$ precipitates have different sizes ranging from several to several tenth nanometers. The surface of the sample is relatively smooth with a RMS of 16.3 nm. Figure 4a is a MFM image taken from the same area from which the AFM image shown in Fig. 3a was taken. The bright and dark areas in the image correspond to

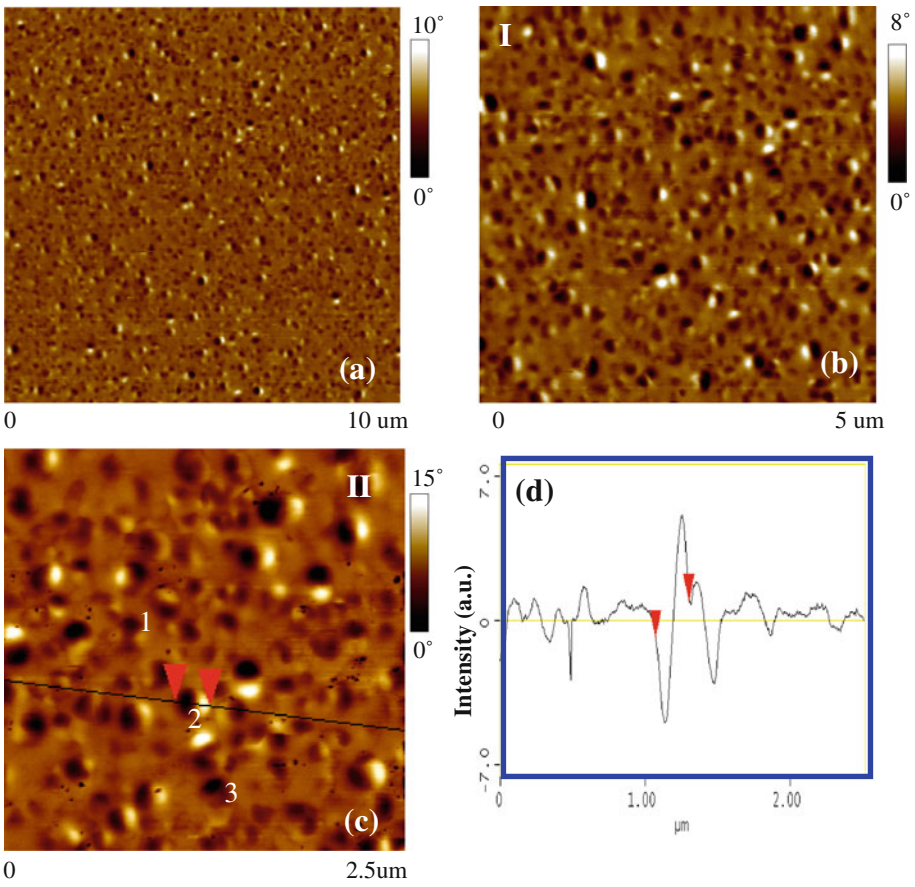

Fig. 4 MFM images acquired at different experimental setting: **a** set-point = 1.323 V, lift height = 45 nm, **b** set-point = 1.323 V, lift height = 35 nm, and **c** set-point = 1.8541 V, lift height = 30 nm, respectively. **d** is a profile of one of the ferromagnetic particles

regions where the magnetic force acting on the MFM tip is repulsive and attractive, respectively. Figure 4b, c is two MFM images taken from the areas outlined in Fig. 3a marked as I and II, respectively. These enlarged MFM images show more clearly the domain structures of the precipitates. Results indicate that one-to-one correspondence can be found between the MFM images and the corresponding AFM images This means that all the particles are ferromagnetic having randomly oriented ferromagnetic domains. Figure 4c shows that there are probably three types of contrasts in the MFM image indicating different magnetic states marked as 1–3, respectively. The type 1 seems to contain two bright–dark pairs that were believed to arise from a magnetic quadrupole [7]. The type 2 shows two symmetrical/asymmetric opposite magnetic poles correspond to single-domain particles whose magnetic moments lie in the surface plane or tilt out-off plane a little bit, respectively. The type 3 shows dark contrast only that indicates the attractive interaction between the tip and the precipitates, i.e., the magnetic moments of these precipitates paralleling to the tip magnetic direction [7]. Obviously, most of them have single magnetic domains. Figure 4d is a profile of one of the ferromagnetic particles which shows well-symmetrical contrast of the N and S poles of the particle that is in-plane magnetized.

Conclusions

High-temperature RTA-induced formation of ferromagnetic $Fe_3Ga_{2-x}As_x$ precipitates in the top surface of GaAs. The sizes of these nanoparticles are from several to several hundred nanometers. The precipitates were confirmed to have two different orientation relationships to the GaAs matrix and most of them have single-domain structures with randomly oriented magnetic pole directions.

Acknowledgements The JEOL-2010F STEM/TEM used for this study was funded by NSF through the Grant DMR-9871177 and operated by the EMAL at the University of Michigan.

References

1. Prinz GA (1990) Science 250:1092
2. Bader SD (2006) Rev Mod Phys 78:1
3. Ohno H (1998) Science 281:951
4. Prinz GA (1990) Science 282:1660
5. Awshalom DD, Flatte ME (2007) Nat Phys 3:153
6. Chang JCP, Otsuka N, Harmon E, Melloch MR, Woodall JM (1994) Appl Phys Lett 65:2801
7. Shi J, Kikkawa JM, Proksch R, Schaffer T, Awschalom DD, Medeiros-Ribeiro G, Petroff PM (1995) Nature 377:707
8. Shi J, Gider S, Babcock K, Awschalom DD (1996) Science 271:937
9. Talut G, Reuther H, Mücklich A, Eichhorn F, Potzger K (2006) Appl Phys Lett 89:161909
10. Theodoropoulou N, Hebard AF, Chu SNG, Overberg ME, Abernathy CR, Pearton SG, Wilson RG, Zavada JM (2001) Appl Phys Lett 79:3452
11. Theodoropoulou N, Hebard AF, Chu SNG, Overberg ME, Abernathy CR, Pearton SG, Wilson RG, Zavada JM (2002) J Appl Phys 91:7499
12. Rahmoune M, Eymery JP (1997) J Magn Magn Mater 165:237
13. Spangenberg M, Neal JR, Shen TH, Morton SA, Tobin JG, Waddill GD, Matthew JAD, Greig D, Malins AER, Seddon EA, Hopkinson M (2005) J Magn Magn Mater 292:241
14. Shaw JW, Falco CM (2007) J Appl Phys 101:033905
15. Harris IR, Smith NA, Cockayne B, MacEwan WR (1987) J Cryst Growth 82:450
16. Harris IR, Smith NA, Delvin D, Cockayne B, MacEwan WR, Longworth G (1989) J Less Common Met 146:103
17. Cockayne B, Olivier PE, Lane PA, Wright PJ, Smith NA, Harris IR (1995) J Cryst Growth 148:261
18. Députier S, Guérin R, Guivarc'h BEA, Jézéquel G (1997) J Alloys Compd 262–263:416
19. Lépine B, Lallaizon C, Schieffer P, Guivarc'h A, Jézéquel G, Rocher A, Abel F, Cohen C, Députier S, Nguyen Van Dau F (2004) Thin Solid Films 446:6
20. Hartmann U (1999) Annu Rev Mater Sci 29:53
21. Sun K (2002) Acta Mater 50:3709